

Growth α -Fe₂O₃ nanowires with different crystal direction of iron film

Li-Chieh Hsu, Yuan-Yao Li*

Department of Chemical Engineering

National Chung Cheng University, 168 University Rd., Min-Hsiung, Chia-Yi 621, TAIWAN, R.O.C

*Corresponding Author: Yuan-Yao Li, E-mail: chmyyl@ccu.edu.tw

ABSTRACT

α -Fe₂O₃ nanowires (NWs) were synthesis from different crystal direction of iron film by thermal oxidation in oven. The crystal direction of iron film was successfully control by sputtering 50 nm iron on different direction of MgO substrate. The directions of MgO substrate were (100), (110) and (111). The crystal direction of coated iron film would follow the direction of the MgO. The NWs were fabricated on the directions of (211) and (110) iron film for 10 hours at 350 °C. The α -Fe₂O₃ NWs with the diameter of 10–30 nm and 1 μ m in length were observed. The α -Fe₂O₃ film was formed on the direction of Fe(100) film after thermal process. The samples were observed and analyzed by field emission scanning electron microscopy (FE–SEM), transmission electron microscopy (TEM) and X–ray diffraction (XRD).

Keywords: α -Fe₂O₃ nanowires

1 INTRODUCTION

α -Fe₂O₃ (hematite) is a semiconductor ($E_g=2.1\text{eV}$) and the most stable iron oxide under ambient environment.[1] The applications of α -Fe₂O₃ nanomaterial were extensively studied for water splitting,[2,3] gas sensor,[4-6] photocatalysts/catalyst,[7-9] solar cell,[10] field emission devices[11,12] and field effect transistors (FET).[13] In addition, the magnetic property of α -Fe₂O₃ crystal also attracts many attentions.[14-17] This is because crystalline α -Fe₂O₃ has the characteristic of antiferromagnet with a Neel temperature (T_N) at 960 K and a Morin temperature (T_M) at 263 K which a magnetic phase will be transited.[18] When the temperature is between T_N and T_M , the weak ferromagnetic property of α -Fe₂O₃ is observed.[19,20] Many methods have been developed for the fabrication of α -Fe₂O₃ nanowires (NWs) or nanorods including template methods,[14,21] hydrothermal,[18,22,23] and sol-gel mediated reaction,[24] as well as the thermal oxidation of iron.[12,25-27] The thermal oxidation methods normally used a mixture of gas (O₂, CO₂, N₂, SO₂ or H₂O) or air in the synthesis process and the temperature of oxidation is from 300–700°C within few hours. After the process, α -Fe₂O₃ NWs or nanorods can be grown on the bulk of pure iron.

In general, the growth mechanism of α -Fe₂O₃ NWs was preferred to the tip-growth[25]. The α -Fe₂O₃ NWs were formed on the defect of the Fe film by the diffusion of the oxygen. In previously surveys, most researches were investigated the influence of the grown α -Fe₂O₃ NWs, including the keeping temperature, the gas conditions, the holding time, ...et al.. In this study, the NWs were grown on the 50 nm thick iron film at 350 °C for 10 hours. In order to analyze the growth mechanism of the α -Fe₂O₃ NWs, the iron films were sputtering on the three different crystal directions of the MgO substrates. The deposited directions of the Fe films were affected with the crystal directions of the MgO substrates. This is the first time to investigate the relationship between the crystal direction of the Fe film and the growth of the α -Fe₂O₃ NWs. We reported the results in this paper, the α -Fe₂O₃ NWs were grown on the directions of the Fe (211) and Fe (110). As the direction of Fe film was (100), only the α -Fe₂O₃ film was formed after thermal process.

2 EXPERIMENTAL

α -Fe₂O₃ NWs were grown by iron film using the thermal oxidation at 350°C for 10hours. The 50 nm thickness of Iron film was coated on the MgO substrate by direct current (DC) sputtering. The directions of MgO substrate were (100), (110) and (111), respectively. The various MgO substrates were placed into a DC sputter machine, and it was coated while the pressure was achieving 10⁻⁶ torr. The target was 99.9 % of pure iron. The iron-coated substrates were heated at 350 °C for 10 hours in an oven at the ambient environment. The morphology and the structure of the as-synthesized NWs were characterized by field emission scanning electron microscopy (FE–SEM, HITACH S–4800) and high resolution transmission electron microscopy (HR–TEM, JEOL JSM 3010), respectively. The crystal directions of NWs or films are identified by X–ray diffraction (XRD, RIGAKU Miniflex system using a Cu target, $\text{CuK}\alpha = 1.5418 \text{ \AA}$) spectrometer.

3 RESULTS AND DISCUSSION

Figures 1(a) and 1(b) show the top-view and cross-section of the Fe-coated MgO(110) after thermal oxidation at 350 °C for 10 hours, respectively. As can be seen in

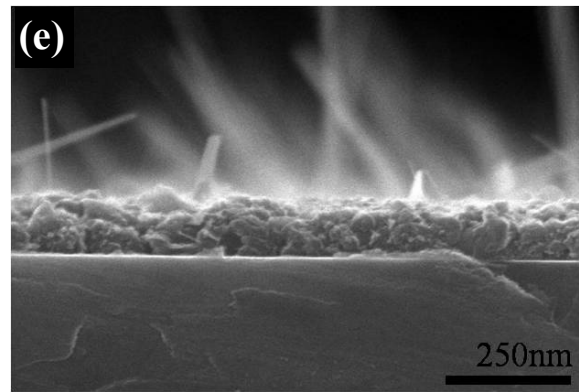
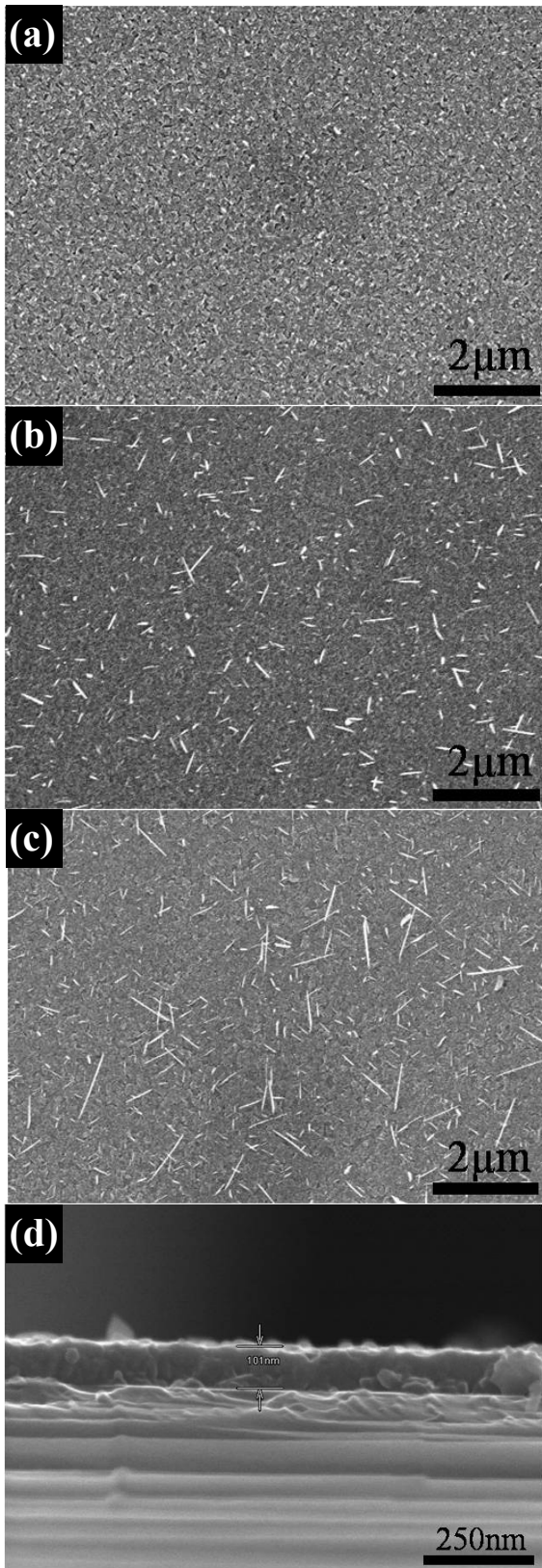


Figure 1: The FE-SEM images of the top view of the Fe-coated (a) MgO(100), (b) MgO(110) and (c) MgO(111) after thermal treatment, the cross-section view of the film Fe-coated (d) MgO(100) and (e) MgO(111) after thermal treatment.

Figure 1(a), there are no wire-like structure on the surface of the film. The morphology of the film was porous structure and very roughly. Figure 1(d) shows the thickness of the film was 100 nm after thermal oxidation. There are no wire-like structures on the surface of the film. Figures 1(b) and 1(c) show the top-view of the Fe coated MgO(110) and MgO(111) substrate. The NWs were grown vertically on the MgO(110) and MgO(111) substrates with the diameters of 10–30 nm and the lengths of 1 μm. The porous structures were found on the surface of the films. As can be seen in Figure 1(e), the NWs were vertically growth on the surface of the Fe film. The thickness of film was 90 nm.

From Figures 1, we found that, the surface of these films were porous structures. The thicknesses of the films were doubled (~100 nm) compare with the thickness of the original Fe film (50 nm). It is well known that the Fe will be oxidized to α -Fe₂O₃ by the diffusion of oxygen. It could explain that the thickness was thicker after thermal process. The film on the MgO(100) was thicker than the films on the MgO(110) and MgO(111), because of the NWs were grown on the film.

Figure 2(a) shows a TEM image of the NWs. The NWs are very straight with a diameter of 10–30 nm and the length of several hundred nm. The high resolution TEM image shown in Figure 2(b) indicates a well crystalline structure of the α -Fe₂O₃ NW with growth direction along [110]. The fringe spacing of 0.251 nm agrees well with the interplanar spacing of (110) of the α -Fe₂O₃ NW. In Figure 2(c), the selected area electron diffraction (SAED) pattern reveals that the crystal structure of the α -Fe₂O₃ NW is the single rhombohedral structure.

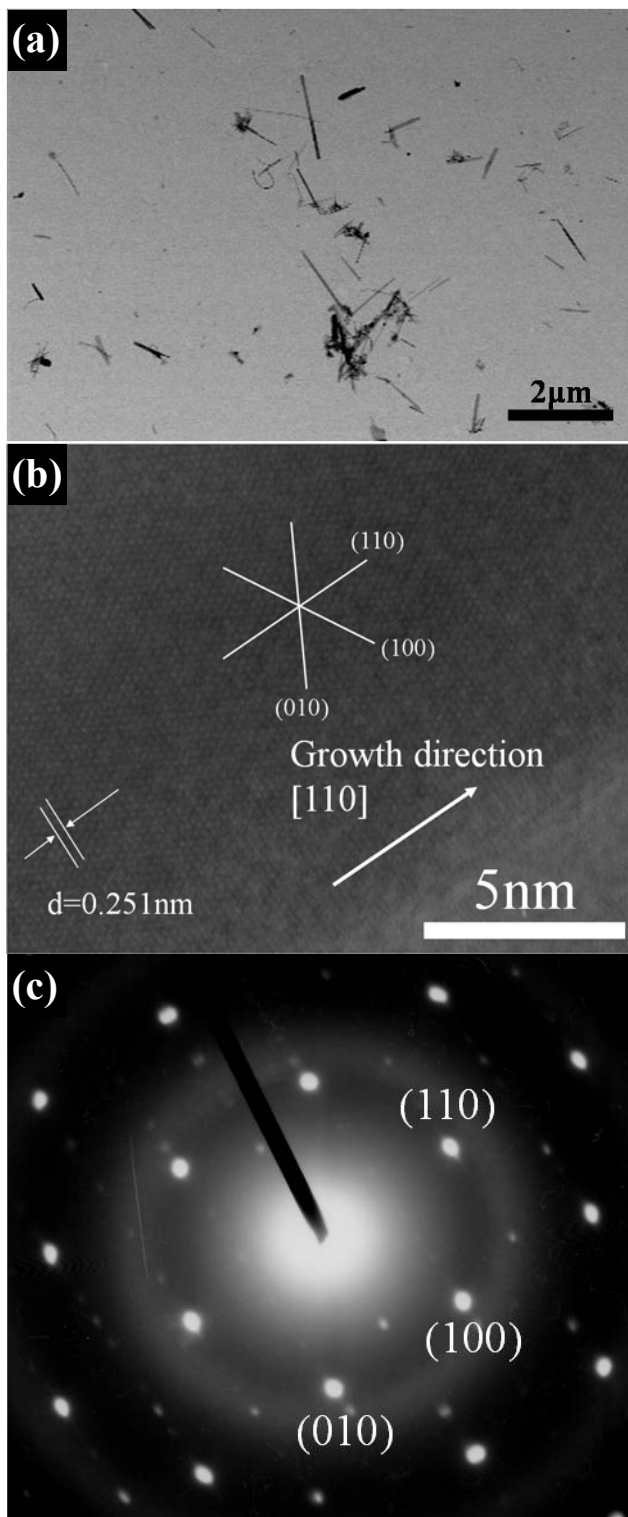


Figure 2: (a) TEM image of the α -Fe₂O₃ NWs, (b) HR-TEM image of the single α -Fe₂O₃ NW, (c) SAED pattern of the α -Fe₂O₃ NW.

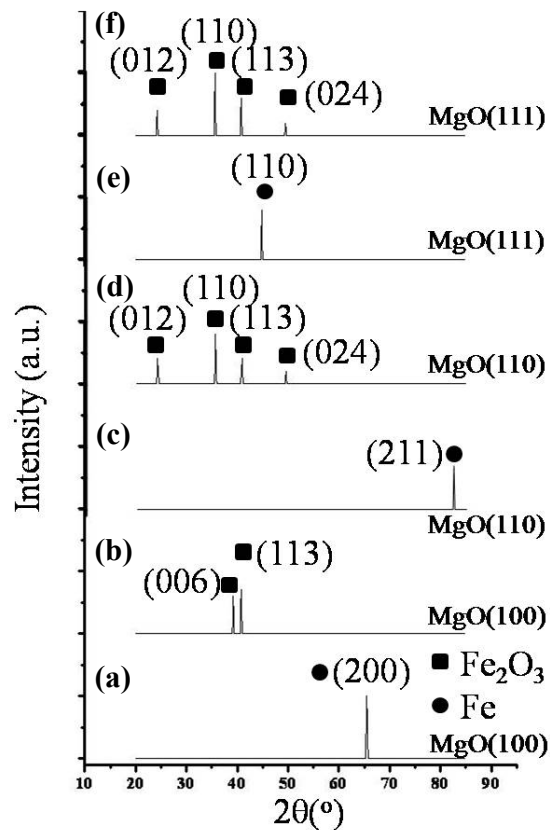


Figure 3: The XRD patterns of Fe-coated MgO(100) (a) before oxidation and (b) after oxidation, MgO(110) (c) before oxidation and (d) after oxidation, and MgO(111) (e) before oxidation and (f) after oxidation.

The XRD patterns of the various Fe-coated MgO substrates were shown in Figure 3. It can be seen that the XRD patterns of the samples are in conformity with rhombohedral α -Fe₂O₃ after thermal treatment. As shown in Figures 3(a) and 3(b), the crystal direction of the Fe film coated on the MgO(100) substrate was (100). The α -Fe₂O₃ peaks of the diffraction planes (006) and (113) were appeared after thermal process. Figures 3(c) and 3(d) shows the Fe(211) was deposited on the MgO(110) substrate. After oxidation, the α -Fe₂O₃ of the (110), (113) and (012) diffraction peak are clear distinguishable. In Figure 3(e), the crystal direction of Fe film coated on the MgO(111) substrate was (110). The α -Fe₂O₃ diffraction peaks of the (110), (113) and (012) were shown in Figure 3(f). From the XRD patterns, the various crystal directions of Fe films were formed by the different directions of the MgO substrates. The three crystal directions of Fe films were oxidized to α -Fe₂O₃. This is the reason why the surfaces of the films we found were porous structures in Figures 1. According to the analysis of the XRD and TEM, the NWs were grown on the Fe film while the crystal direction of α -Fe₂O₃(110) was formed. This is good agreement with the result of the reference.[25] Compared with the Fe(100), the

oxygen was easier diffused along the Fe(110) on the surface of the Fe(211) film and Fe(110) film. The films of Fe(211) and Fe(110) were fabricated the α -Fe₂O₃ NWs after the thermal oxidation.

4 CONCLUCTIONS

α -Fe₂O₃ NWs were synthesis from various crystal directions of iron films by thermal oxidation in oven. The crystal direction of iron film was successfully control by sputtering 50 nm iron on different direction of MgO substrate. The directions of MgO substrate were (100), (110) and (111). The crystal direction of coated iron film would follow the direction of the MgO. The NWs were fabricated on the directions of (211) and (110) iron film for 10 hours at 350 °C. The α -Fe₂O₃ NWs with the diameter of 10–30 nm and 1 μ m in length were observed. The α -Fe₂O₃ film was formed on the direction of (100) iron film after thermal process. Form the results of the XRD and TEM, the NWs were grown on the Fe film while the crystal direction of α -Fe₂O₃(110) was formed. Compared with the Fe(100), the oxygen was easier diffused along the Fe(110) on the surface of the Fe(211) film and Fe(110) film. The controlled growth of the α -Fe₂O₃ NWs promises the more applications in the electrical devices.

5 REFERENCES

- [1] R. Dieckmann, *Philos. Mag. A*, 68, 725-745, 1993.
- [2] I. Cesar, A. Kay, J. A. G. Martinez and M. Gratzel, *J. Am. Chem. Soc.*, 128, 4582-4583, 2006.
- [3] J. H. Kennedy and M. Anderman, *J. Electrochem. Soc.*, 130, 848-852, 1983.
- [4] P. Chauhan, S. Annapoorni and S. K. Trikha, *Thin Solid Films*, 346, 266-268, 1999.
- [5] E. Comini, V. Guidi, C. Frigeri, I. Ricco and G. Sberveglieri, *Sens. Actuators, B*, 77, 16-21, 2001.
- [6] J. S. Han, T. Bredow, D. E. Davey, A. B. Yu and D. E. Mulcahy, *Sens. Actuators, B*, 75, 18-23, 2001.
- [7] B. C. Faust, M. R. Hoffmann and D. W. Bahnemann, *J. Phys. Chem.*, 93, 6371-6381, 1989.
- [8] S. N. Frank and A. J. Bard, *J. Phys. Chem.*, 81, 1484-1488, 1977.
- [9] T. Ohmori, H. Takahashi, H. Mametsuka and E. Suzuki, *Phys. Chem. Chem. Phys.*, 2, 3519-3522, 2000.
- [10] N. Beermann, L. vayssieres, S. E. Lindquist and A. Hagfeldt, *J. Electrochem. Soc.*, 147, 2456-2461, 2000.
- [11] T. Yu, Y. W. Zhu, X. J. Xu, K. S. Yeong, Z. X. Shen, P. Chen, C. T. Lim, J. T. L. Thong and C. H. Sow, *Small*, 2, 80-84, 2006.
- [12] Y. W. Zhu, T. Yu, C. H. Sow, Y. J. Liu, A. T. S. Wee, X. J. Xu, C. T. Lim and J. T. L. Thong, *Appl. Phys. Lett.*, 87, 023103, 2005.
- [13] Z. Y. Fan, X. G. Wen, S. H. Yang and J. G. Lu, *Appl. Phys. Lett.*, 87, 013113, 2005.
- [14] J. J. Wu, Y. L. Lee, H. H. Chiang and D. K. P. Wong, *J. Phys. Chem. B*, 110, 18108-18111, 2006.
- [15] C. Z. Wu, P. Yin, X. Zhu, C. Z. OuYang and Y. Xie, *J. Phys. Chem. B*, 110, 17806-17812, 2006.
- [16] C. H. Kim, H. J. Chun, D. S. Kim, S. Y. Kim and J. Park, *Appl. Phys. Lett.*, 89, 223103, 2006.
- [17] L. Liu, H.-Z. Kou, W. Mo, H. Liu and Y. Wang, *J. Phys. Chem. B*, 110, 15218-15223, 2006.
- [18] Y. M. Zhao, Y.-H. Li, R. Z. Ma, M. J. Roe, D. G. McCartney and Y. Q. Zhu, *Small*, 2, 422-427, 2006.
- [19] Y. L. Chueh, M. W. Lai, J. Q. Liang, L. J. Chou and Z. L. Wang, *Adv. Funct. Mater.*, 16, 2243-2251, 2006.
- [20] M. F. Hansen, C. B. Koch and S. Morup, *Phys. Rev. B*, 62, 1124-1135, 2000.
- [21] J. Chen, L. N. Xu, W. Y. Li and X. L. Gou, *Adv. Mater.*, 17, 582-586, 2005.
- [22] Z. Y. Sun, H. Q. Yuan, Z. M. Liu, B. X. Han and X. R. Zhang, *Adv. Mater.*, 17, 2993-2997, 2005.
- [23] L. Vayssieres, C. Sathe, S. M. Butorin, D. K. Shuh, J. Nordgren and J. H. Guo, *Adv. Mater.*, 17, 2320-2323, 2005.
- [24] K. Woo, H. J. Lee, J. P. Ahn and Y. S. Park, *Adv. Mater.*, 15, 1761-1764, 2003.
- [25] X. Wen, S. Wang, Y. Ding, Z. L. Wang and S. Yang, *J. Phys. Chem. B*, 109, 215-220, 2005.
- [26] Y. Fu, J. Chen and H. Zhang, *Chem. Phys. Lett.*, 350, 491-494, 2001.
- [27] L.-C. Hsu, Y.-Y. Li, C. G. Lo, C. W. Huang and G. Chern, *Appl. Phys. Lett.*, 2008.(submitted)